



DEVELOPMENT OF MODULAR CONNECTIONS FOR STEEL SPECIAL MOMENT FRAMES

Ali SUMER¹, Yong PAN¹, Ge WAN¹, Robert B. FLEISCHMAN²

SUMMARY

Modular connections have been developed for use in seismic-resistant steel moment frames. The connections are engineered specifically to meet performance requirements corresponding to optimal seismic response. The versatility in design required to accomplish this task is not readily available with traditional rolled shapes. Thus, the designs rely on advancements in casting technology to create connections specifically configured for seismic performance.

The impetus for developing the modular connections is the recently discovered susceptibility to fracture of welded connections in steel special moment frames (SMFs) during earthquakes. The consensus from subsequent research on steel moment connections is that an effective earthquake-resistant connection design should be based on a combination of weld fracture mitigation measures and changes of connection configuration aimed at reducing the stress levels or redirecting the stress flow in the connection. Thus, major features of the modular connections are both the minimization of stress/strain and the removal of the field weld from the critical cross-section.

To date, three prototypes have been developed: (1) a panel zone dissipator modular node (PZ-MN); (2) a plastic hinge dissipator modular node (PH-MN), and (3) a bolted modular connector (MC). The PZ-MN dissipates energy through stable panel zone yielding without column kinking and no weld distress; the PH-MN dissipates energy through a contained plastic hinge region; and the MC dissipates energy in a variable-arm connector that minimizes plastic strain demand and eliminates prying forces.

Final designs were developed through a comprehensive analytical investigation of trial configurations and key parameters using nonlinear (material and geometry) finite element analysis. Full-scale prototypes were cast and tested under the FEMA-350 protocol. These connections exhibited excellent performance in terms of energy dissipation, stability and ductility; far exceeding qualifying drift capacities.

¹ Res. Asst., Dept. of Civ. Eng. and Eng. Mech., Univ. of Arizona (UA), Tucson, AZ 85721-0072, USA.
Email: asumer@email.arizona.edu

² Asst. Prof., Dept. of Civ. Eng. and Eng. Mech., Univ. of Arizona (UA), Tucson, AZ 85721-0072, USA
Email: rfleisch@enr.arizona.edu

INTRODUCTION

Modular connections have been developed for use in seismic-resistant steel moment frames. The connections are configured specifically for optimal seismic response. Traditional rolled shapes, developed for use as main structural members, may not possess the necessary geometries to meet this objective. Therefore, the designs rely on the versatility afforded by the casting process to create the forms. The impetus for developing the modular connections is the recently discovered susceptibility to fracture of welded connections in steel special moment frames (SMFs) during strong earthquakes (Malley [1]). The consensus from subsequent research (FEMA-350 [2]) on this topic is that an effective earthquake-resistant connection design should be based on a combination of weld fracture mitigation measures and changes of connection configuration aimed at reducing the stress levels or redirecting the stress flow in the connection (Stojadinovic et al [3]). The cast forms attempt to address these recommendations directly.

Three connection prototypes have been fully developed: a panel zone dissipator modular node (PZ-MN), a plastic hinge dissipator modular node (PH-MN) and a modular connector (MC) (See Fig. 1). A comprehensive research program guided their development including interdisciplinary (steel construction, design consultants, steel foundries, university researchers) meetings to determine promising concepts, evaluation of these concepts through extensive nonlinear finite element (FE) solid modeling analysis, prototype development in conjunction with industry partner oversight, and experimental verification. For the latter, prototypes were cast and fabricated into structural subassemblages and tested in full-scale. In these tests, the connection prototypes exhibited remarkable ductility, repeatability, and enhanced energy dissipation characteristics.

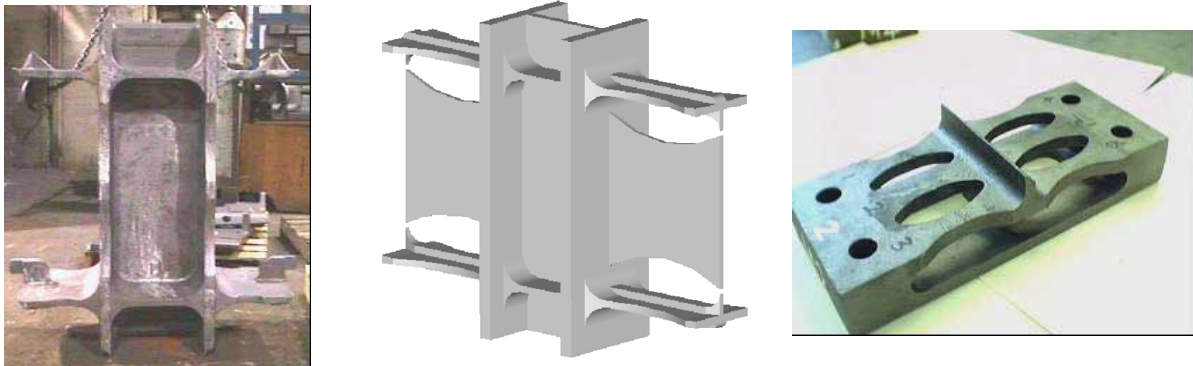


Figure 1. Cast steel Prototypes: (a) PZ-MN; (b) PH-MN (schematic) and (c) MC.

CONNECTION PROTOTYPE DEVELOPMENT PROGRAM

The development of the modular seismic resistant connections involved three steps: (1) Analytical evaluation, (2) Prototype creation, and (3) Experimental verification.

Analytical Research Program

The modular connections were developed through an extensive analytical research program using nonlinear finite element (FE) analysis (ANSYS [4]). Aspects of modeling used to properly characterize the behavior include material nonlinearity, large deformation (updated orientation and true strain) and changing contact conditions. The first stages of the development process involved simple elastic models to assess the potential of certain rough concepts. Once a concept was deemed promising, two-dimensional (2D) FE models (See Fig. 2a) were used to rapidly evaluate parameters and develop the basic form of the prototypes. At this point, three-dimensional (3D) solid models were used for verification of the 2D-FE models and for capturing behavior not possible in the 2D-FE models such as shear lag, triaxial stress states, and out-of-plane stability.

Creation of Prototypes

As the connection configuration took shape, issues of castability had to be addressed. Steel castings find widespread use as structural components in heavy industry applications that are safety critical, performance demanding (often subject to impact or sustained pressure) and in harsh environments (Monroe [5]). However, this application likely marks the first time castings have been required to develop ductility. Identical material to rolled steel (in terms of chemical composition and mechanical properties) can be used in the casting process, however these properties only represent the quality of the steel, and not necessarily the quality of the castings itself. Casting integrity is determined by solidification conditions that are heavily influenced by piece shape, size and wall thickness. The challenge to the foundry engineers (industry partner Varicast) was to meet the structural shape and performance requirements while maintaining an integral casting, requirements that are often at odds.

The geometries desirable for the modular connections such as thin-to-thick transitions or isolated flanges require the careful placement of a number of gravity-driven liquid feed metal reservoirs, termed risers, to compensate volumetric contraction thus avoiding internal shrinkage cavities. Furthermore, the cores within the casting molds used to create internal details must be of sufficient size to dissipate the required density of heat and resist buoyancy forces. Traditionally, this quality control was an a posteriori activity, including mechanical testing, chemical spectography, and non-destructive evaluation. For this research, recent advances in computer simulation of the casting solidification provided the opportunity to perform quality control a priori. For this, the research took advantage of the already created three-dimensional solid models. Through the electronic exchange of CAD files exported by ANSYS, industry partner Varicast and the researchers were able to rapidly arrive at feasible geometries by iterating between structural and thermodynamic/fluid flow FE analysis (See Fig. 2b).

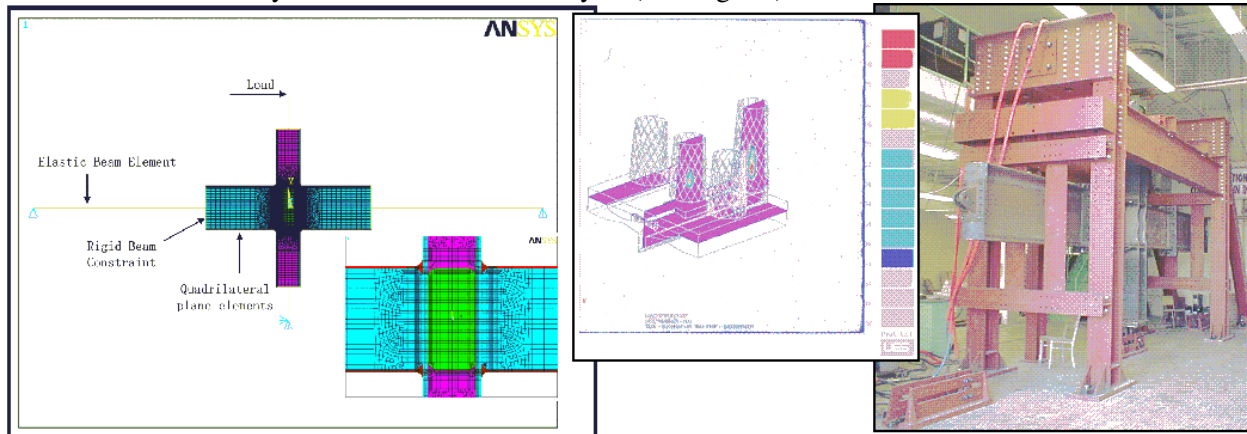


Figure. 2. Research tools: (a) FE analysis; (b) solidification studies, and (c) full-scale experimentation.

Experimental Verification

Once designs were finalized, full-scale prototypes were cast at the Varicast foundry. Industry partner Able Steel developed a welding procedure specification (WPS). Using this WPS, Able fabricated a full-scale subassembly (column with one- and two-sided beam connections). These subassemblies were tested under the FEMA-350 protocol in the large-scale reaction frame at the UA ICEL high bay (See Fig. 2c).

PANEL ZONE DISSIPATOR MODULAR NODE (PZ-MN)

The modular node concept involves a cast piece that is shop welded to the column and field welded to the beam. The Panel Zone Dissipator modular node (PZ-MN) provides a majority of seismic energy dissipation through yielding of the panel zone. The PZ-MN (See Fig. 3a) therefore employs a weak panel zone relative to other components (the beam, column, and “link” region). The panel zone region has long

been recognized as a stable energy dissipation source for SMFs with excellent hysteretic characteristics (Schneider and Amidi [6]) and positive ramifications for frame stability (Krawinkler and Gupta [7]). However, significant panel zone plastic deformation can be detrimental to conventional connection performance because local curvature (“kinking”) of the column flange at the interface with the beam flange (See dashed line in Fig. 3b) produces a high fracture potential at the weld location (El-Tawil [8]). In fact, the recent trend has been to design against weaker panel zones (Engelkirk [9]). Thus to accomplish a viable PZ-MN design, column kinking must be mitigated. Several features combine to meet this objective and also to minimize stress at the beam interface (Fleischman and Li [10]):

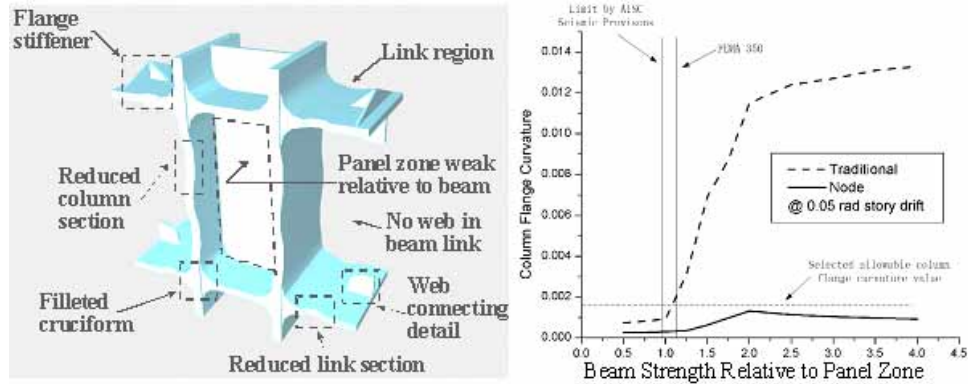


Figure 3. PZ-MN: (a) prototype configuration; and (b) column curvature.

Stable Panel Zone Yielding

Gradually increasing sections, termed filleted cruciforms (See Fig. 3a), are cast into the flange intersections. The cruciforms reduce the column flange kinking during large panel zone plastic distortion (See solid line in Fig. 3b). It is important to note that these details would be extremely costly and difficult to fabricate. On the other hand, the incorporation of the cruciforms in a casting is trivial, in fact their presence actually improve the integrity of the casting. The mitigation of kinking effects and the removal of the field weld eliminate the potential for fracture at the column face.

Joint Mechanism

The cruciforms permit stable behavior of the intentionally weak panel zone. However, their high local stiffness exacerbates restraint in the web near the beam-column flange interface. Fig. 4a indicates (for an early PZ-MN version) that because of this restraint, the maximum strain demand exists outside the panel zone, thus compromising the design objective. Web restraint is further detrimental for weak panel zones because it significantly amplifies the beam flange shear. Thus, a link region was conceived that carries the beam shear solely within the flange itself, enabling the elimination of the web, and together with the rather straightforward insertion of purposeful weak sections into the flanges of the casting (Fig. 4b), forms a ductile joint mechanism (Fig. 4c).

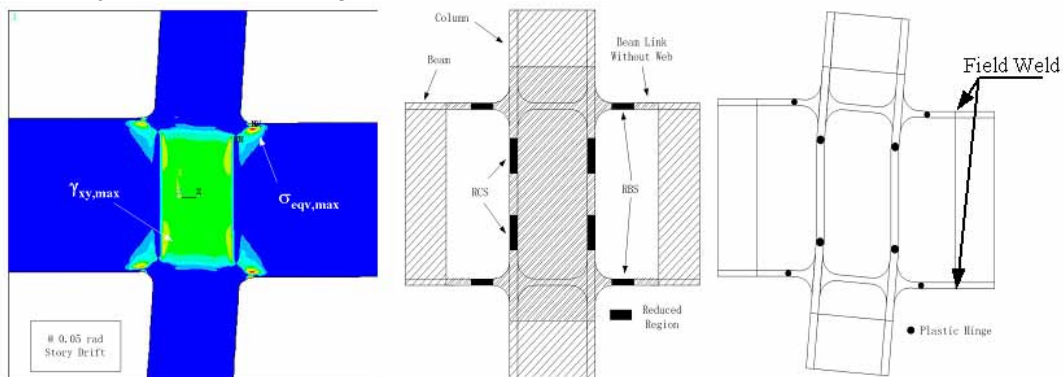


Figure 4. (a) Plastic strain for early PZ-MN; (b) link design; (c) joint mechanism.

Weld Stress Mitigation Features

Even in achieving the joint mechanism shown in Figure 4c, local (secondary) bending of the flange places unwanted demands on the field weld to the beam. The single line geometry of this weld provides little leverage against these bending stresses. Fortunately, a flange stiffener easily cast into the node eliminates secondary bending at the field weld location, (FE results indicate a reduction of weld stress from $1.7M/S_x$ to $1.03M/S_x$). A web connection detail stabilizes the beam link flange by providing moment of inertia to the weld. The web connecting detail also provides a location for placing erection bolts.

PZ-MN Experimental Verification

A full-scale PZ-MN prototype was cast (Refer to Fig. 1a) and fabricated into subassemblages containing large WF sections. These subassemblages were tested monotonically and cyclically using the FEMA-350 load protocol (See Table 1). The full joint mechanism anticipated by the FE analysis was observed in the experiments (See Fig. 5). Fig. 6a shows the monotonic results. At the test conclusion (0.18 rad), the node and welds exhibited no distress. Fig. 6b indicates remarkable cyclic performance: the PZ-MN specimen reached the actuator stroke limit (± 0.077 rad) with no distress, well beyond the FEMA-350 acceptance drift. The specimen was cycled an additional 12 times at this displacement before a low-cycle fatigue failure formed in the panel zone. Neither the shop welds at the column interface nor the field welds at the beam interface suffered distress and gages indicated elastic behavior at these sections. Comparison with the monotonic envelope shown in Fig. 6b indicates the incredible level of cyclic work. Both plots indicate good agreement with analytical predictions.

Table 1. PZ-MN Full Scale Test Descriptions

Test ID	Type of Loading	Column	Inner Beam	θ_u (rad)
PZ-MN-1	Monotonic	W14x193	W30x99	0.18
PZ-MN-2	Cyclic (FEMA350)	W14x193	W30x99	0.077 (14 cycles)
PZ-MN-3	Cyclic (Gravity load = 890 kN)	W14x193	W30x99	0.077 (7 cycles)

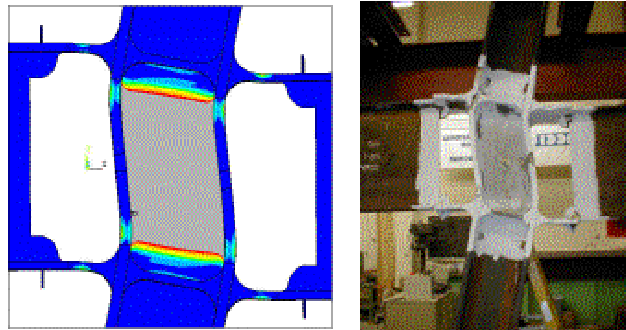


Figure 5. Development of joint mechanism:(a) analysis; (b) full-scale

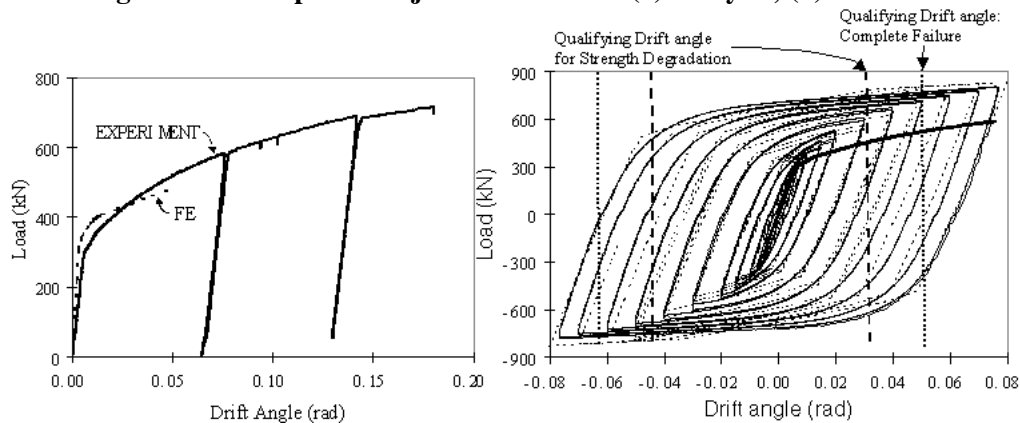


Figure 6. Experimental and analytical: (a) monotonic (b) cyclic experiment.

A subsequent full-scale subassembly test was performed with gravity load simulated by post-tensioning prestressing cables as shown in Fig. 7. The PZ-MN tested with superimposed gravity load exhibited the same anticipated mechanisms as in previous tests. The low cycle fatigue life, though reduced, was still well above FEMA-350 acceptance criteria (See Table 1).



Figure 7. Cyclic PZ-MN test with gravity load: (a) undeformed; and (b) deformed.

Analytical Model of PZ-MN For Ground Motion Simulations

To evaluate the seismic performance of the PZ-MN, a benchmark special moment frame (SMF) from the SAC project [11] was redesigned for the PZ-MNs following IBC-2000 guidelines [12]. The SMF design is typically controlled by drift limits. Therefore, the nominal strength (ϕM_p) of its girders is typically much greater than the required seismic design moments. PZ-MN structures, in which the joint strength and beam stiffness are uncoupled, can be designed for a strength near the design force. It was therefore desired to see if it is feasible to design these efficient and ductile connections with less than the typical overstrength of the traditional frames.

Using the 3D FE results, a simple model of the PZ-MN is constructed in ANSYS (See Fig. 8a). The link elements representing the panel zone consist of multi-linear kinematic strain hardening (MKIN) and multi-linear isotropic strain hardening (MISO) material models in parallel to capture the hardening cyclic behavior. Comparison of this finite element model and the test results are shown in Fig. 8b, indicating adequate accuracy. A bilinear (2% hardening) model is used for the traditional connection. The models were subjected to two suites of acceleration time histories corresponding to ground motions having probabilities of exceedance of 10% and 2% in 50 years for the Los Angeles region [13]. Interstory drift angle and cumulative plastic rotation are chosen as the primary seismic demand parameters.



Figure 8. Dynamic model: (a) Simplified joint model; (b) Load vs. drift comparison w/experiment

The response of the traditional SMF design and the PZ-MN design are compared in Fig. 9. Despite the lower strength design of the PZ-MN structures, similar drift demands are obtained in comparison to the traditional structures. Furthermore, the non-degrading model used for the traditional SMF is highly idealized, and in reality, the stiffness and strength deterioration common for traditional connections may have some adverse effects on the story drift demands. On the contrary, the PZ-MN gathers strength as its ductility demand increases, and with little potential for early fracture, greatly reduces the possibility of collapse under severe earthquakes.

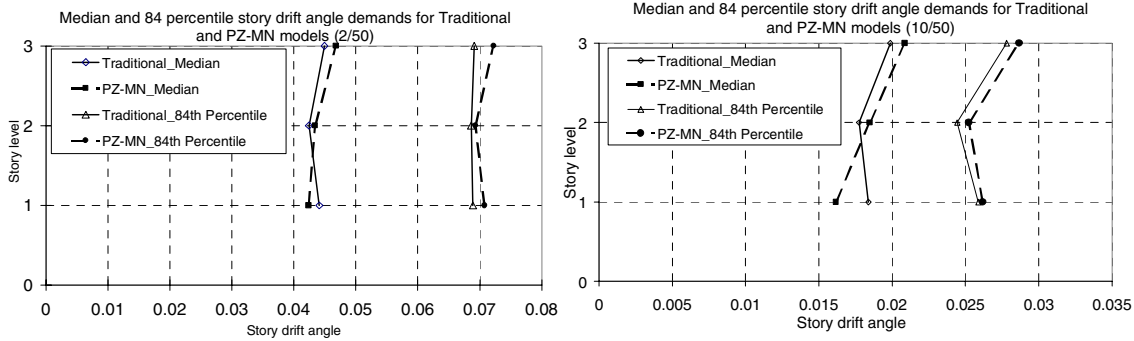


Figure 9. Interstory drift angle comparisons for (a) 10/50, and (b) 2/50

Coffin-Manson [14] fatigue life expressions similar to those developed elsewhere (Richard et al [15]) for traditional and slotted web connections are defined for the PZ-MN using an approximate curve fit of the experimental data. These expressions relating story drift (θ) amplitude to N_f is the number of cycles to failure are shown in the header of Table 2. Fatigue life is predicted by applying rainflow counting methods to the highly irregular story drifts histories produced by a ground motion, and tabulating the results with a Palmgren-Miner rule [15]. Expected life data for the 1985 Vina del Mar (Chile) ground motion scaled to 0.8g PGA (PEER) is tabulated in Table.2.

Table 2.

Interstory Drift Range	1985 Vina del Mar (3rd floor)							
	TRAD			SLWB			PZMN	
	$N_f = e^{(3.34-drift)/0.55}$ [15]	Cycles n	$\frac{n}{N_f}$	$N_f = e^{(4.96-drift)/0.65}$ [15]	$\frac{n}{N_f}$	$N_f = e^{(10.43-drift)/0.9}$	n	$\frac{n}{N_f}$
0.05%~0.25%	361.7	45	0.12	1766.8	0.03	96546.3	51	5.28E-04
0.25%~0.75%	174.8	48	0.27	954.8	0.05	61903.6	51	8.24E-04
0.75%~1.25%	70.4	30	0.43	442.4	0.07	35517.4	21	5.91E-04
1.25%~1.75%	28.4	9	0.32	205.0	0.04	20378.2	12	5.89E-04
1.75%~2.25%	11.4	1	0.09	95.0	0.01	11692.1	2	1.71E-04
2.25%~2.75%	4.6	0	0.00	44.0	0.00	6708.4	1	1.49E-04
2.75%~3.25%	1.9	1	0.54	20.4	0.05	3848.9	0	0.00E+00
			1.77		0.25			0.003

PLASTIC HINGE DISSIPATOR MODULAR NODE (PH-MN)

A Plastic Hinge Dissipator modular node (PH-MN), currently at the prototype testing stage, contains a controlled plastic hinge region and features to mitigate force concentrations, triaxiality and local buckling. The majority of seismic energy dissipation occurs in the node plastic hinge or link region. The PH-MN employs a “balanced” design in which the panel zone contributes a non-negligible portion of the seismic energy dissipation. A capacity design assures that the link is weaker than surrounding structural beams.

A major benefit of the PH-MN design is that the field weld is removed from the critical cross-section at the column face. In traditional welded-flange connections, the field weld acts as a potential source of brittle fracture (FEMA 350 [2]) because: it is difficult to control the weld quality and thus flaws may initiate a crack; a heat affected zone (HAZ) develops in which the properties of the parent material may be compromised; the weld requires a beam web access hole that creates strain concentrations; the weld location is at a region of high triaxial restraint that can suppress yielding in favor of brittle fracture, and, the high forces act in the through-thickness direction of the column flange. The critical cross section in

the PH-MN is, in contrast, structurally continuous and inherently isotropic. A field weld is made at the node/beam interface, a less critical cross-section at which stresses have been evaluated and minimized.

The PH-MN has the following features (See Fig. 10): (1) isolated flanges in the node link region to relieve restraint at the flange/web juncture; (2) reduced flange sections to control the location of flange yielding within the link; (3) integral stiffeners along the link flange to permit a long isolated flange length without significant local buckling; (4) a reduced web section to complete the plastic hinge mechanism without incurring strain concentrations at the web/column interface; (5) a filleted cruciform to reduce triaxiality and column flange kinking; (6) a flared inner stiffener interface that provides a robust field weld and a location for erection bolts.

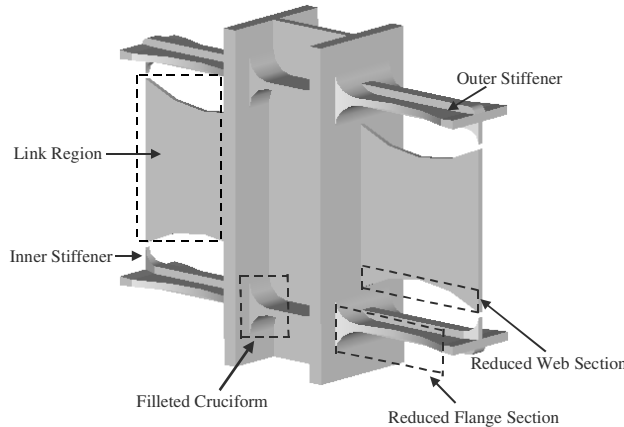


Figure 10. PH-MN Configuration

(1) Link Plastic Hinge Region

The majority of the seismic energy dissipation occurs within the link plastic hinge region. The reduced flange and web sections are easily introduced into the casting, and create a controlled plastic hinge mechanism that keeps the surrounding regions elastic, particularly at the column interface and at the field weld section. The isolated flange design mitigates the high shear force attracted by beam flanges near the column interface. In doing so, the isolated flanges essentially accomplish the objective of other designs (slotted web (Richard et al [16], free flange (Choi et al [17,18])). This high shear has been shown to cause large local bending of the beam flange (Richard et al [16]). Likewise, the reduced flange sections accomplish the intent of the RBS (Engelhardt [19]) though through a modified geometry due to the presence of a continuous cruciform in place of a field weld at the column interface and the lack of a connected web. Note the significant reduction in maximum strain in Fig. 11 created by the use of the reduced web section.

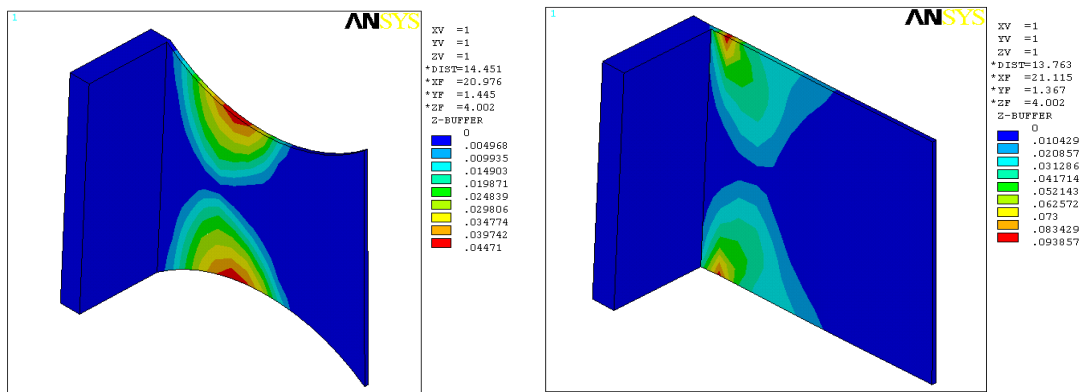


Figure 11. Equivalent plastic strain in link beam web: (a) reduced; (b) prismatic.

(2) Integral Flange Stiffener

Isolating the beam flange from the beam web significantly reduces shear forces in the flange at the column interface. However, the loss of the bracing provided by the web will induce earlier onset of local buckling in the (isolated) compression flange as the PH-MN incurs plastic rotation. Flange local buckling in plastic hinges within a SMF should be avoided as it results in connection strength degradation, which in turn may lead to increases in frame story drifts and severe P- Δ effects. Flange local buckling will also cause high localized strain that may lead to an early onset of low cycle fatigue induced tearing of the beam flanges, which ultimately limits the ability of the assembly to withstand cyclic inelastic rotation demands (FEMA 350 [2]). Therefore, it is desired to suppress the flange local buckling, at least until after the subassembly undergoes large plastic rotation.

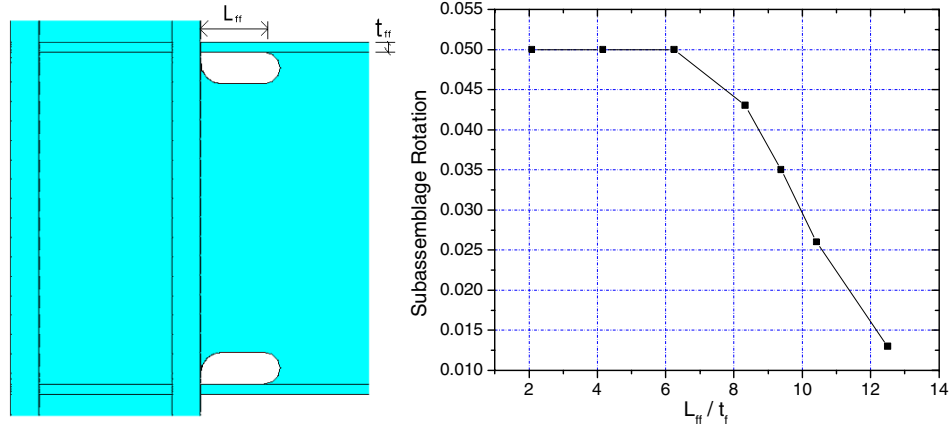


Figure 12. (a) Isolated (free) flange parameters, (b) Rotation demand vs. L_{ff}/t_f

Researchers have advised that the length of an isolated (free) flange be less than 5~6 t_f (Choi et al [17, 18]). Figure 12b, a plot of the rotation at peak load (i.e., the onset of local buckling) for subassembly analyses taken to a maximum of 0.05 rad, shows the veracity of this recommendation. However, the PH-MN design intent is to develop ductility beyond what can be accomplished with traditional sections. In this regard, a free flange length of 6 t_f does not achieve the desired spread of plastic strain. For this reason, an integrated top and bottom stiffener is added along the PH-MN link flange. The stiffener flows into the cruciform at the column face and terminates with an arc at the beam interface. The inner stiffener is tapered and flared for connecting with the web of the surrounding beam. The presence of the stiffener can be used to suppress local buckling of the isolated flange at small plastic rotations. Fig. 13a ($L_{ff}/t_f=21.5$) shows the non-critical level of equivalent plastic strain in the stiffened isolated (compression) flange at 0.05 rad; Fig. 13b indicates no strength degradation in the PH-MN load-displacement relationship.

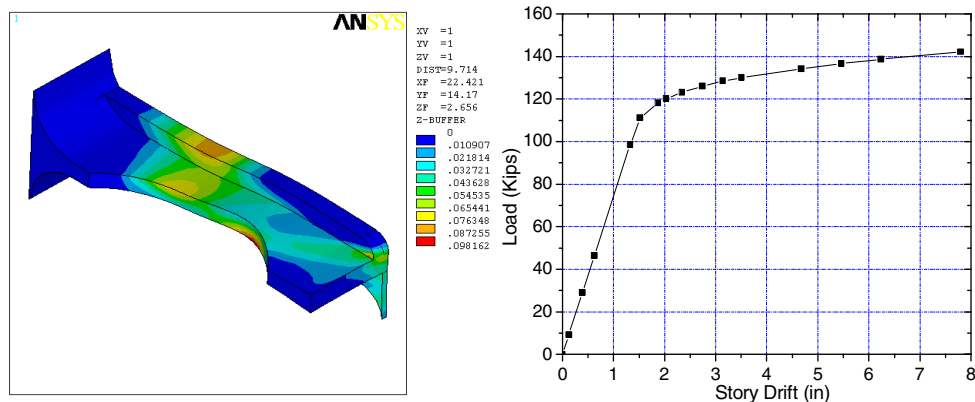


Figure 13. PH-MN: (a) Plastic strain of compression flange; and (b) Load vs. Story Drift

(3) Filleted Cruciform

The filleted cruciform is used to reduce triaxial tension at the PH-MN column/beam flange interface. Triaxiality, defined as the ratio of the maximum principal stress to the Von Mises yield stress, has been cited as one of the potential causes of the welded connection poor performance (Yang and Popov [20]). A comparison of triaxiality between the PH-MN and a traditional connection shows the beneficial effect of the cruciform (See Fig. 14a). It should be further noted that no weld flaws exist at the PH-MN interface.

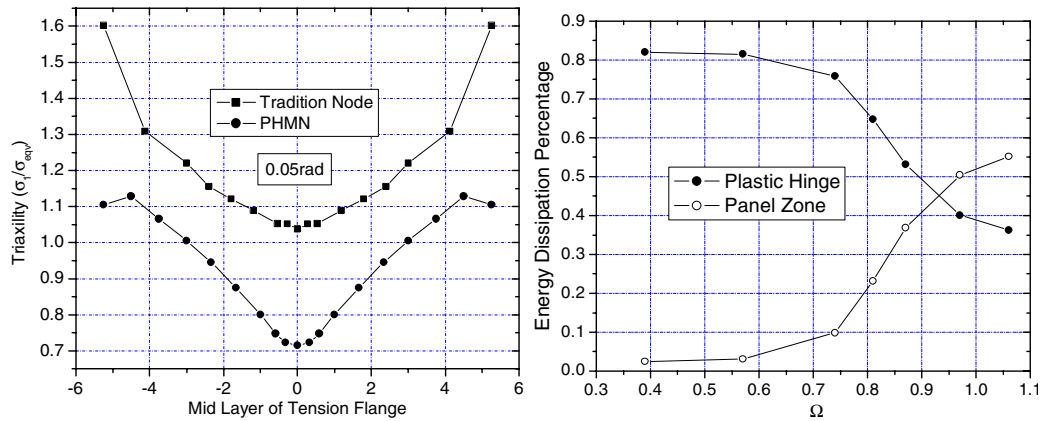


Figure 14. (a) Triaxiality: PH-MN and traditional connection, (b) Panel zone relative strength.

(4) Panel Zone Strength

It is well known that the augmentation of a plastic hinge special detail with energy dissipation in the panel zone reduces the strain demands in the plastic hinge region. Since the PH-MN is continuous across the interface between the panel zone and the plastic hinge region, and thus has none of the issues related to weld, HAZ, triaxiality, and lamellar tearing, it makes sense to exploit the panel zone energy mechanism through a “balanced” design. Fig. 14b shows the energy dissipation percentage with respect to a beam-to-panel zone strength coefficient, Ω . A selection of $\Omega = 0.9$ is made for the balanced PH-MN design. It should be noted that for the PZ-MN, $\Omega = 4.2$.

MODULAR CONNECTOR (MC)

The MC is a cast bolted connector intended as an alternative for full-moment connections. In construction, the MC is to be shop welded to the beam flange and field bolted to the column (See Fig. 15a). Thus the MC connection is similar to the traditional tee-stub connections (Swanson and Leon [21]).

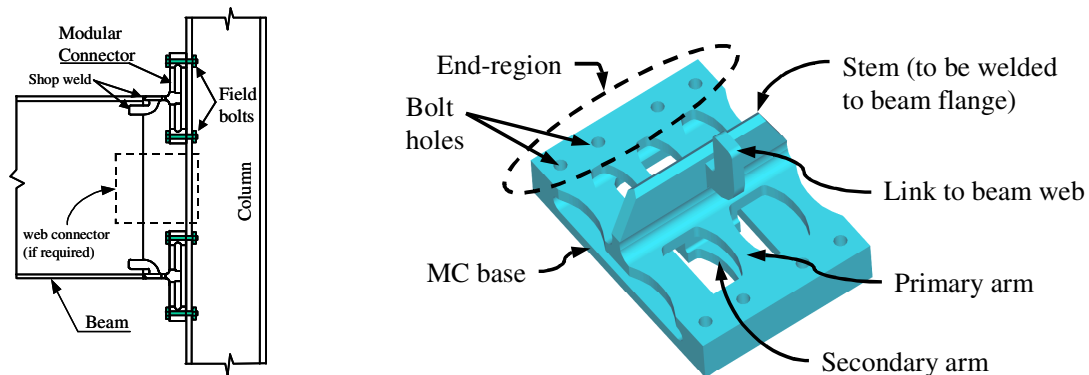


Figure 15. Modular Connector: (a) joint; (b) configuration.

The MC itself is similar in form to structural tee (WT) sections used in tee-stub connections. However, through its unique configuration, it not only improves the efficiency of the fasteners transferring force to the column, it allows ductility to develop within the connector itself, thereby controlling the failure mode

and leaving the main member undamaged. This objective is accomplished through stable yielding of variable width arm elements (See Fig. 15b), an approach used successfully in the past for metal dampers in bracing systems, termed ADAS elements (Whittaker et al. [22]). However, different than the ADAS application is which axial compliance can be built into the device, the desire to diminish slip in the connection results in the need to accommodate catenary forces at large ductility demands (See Fig. 16). An example of the deformed shape of the MC at large (beam end rotation) ductility demand is shown in Fig. 16a. Catenary forces are axial tension forces that develop in flexural members at large deflection due to lengthening (See Fig. 16b). As the MC application must accommodate rather than avoid the catenary forces (Fleischman and Sumer [23]) a different geometry than the ADAS must be adopted. This geometry, shown in Fig. 17, has been engineered to accommodate a complex yield state due to moment, shear and axial force components at a section (See Fig. 16c).

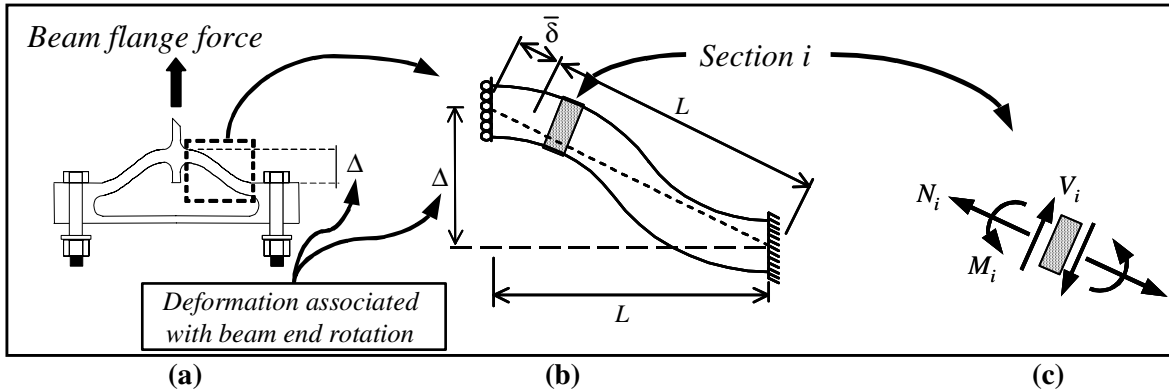


Figure 16. Forces in deformed MC arm

The global properties of the MC (strength, stiffness, etc.) are defined by the geometric parameters shown in Figure 17. Optimum geometry, however, is expressed through geometric ratios: a percentage width reduction $B_{min}/B_{max} = 0.45$; an aspect ratio $L/B_{max} = 2$; a limiting length-to-thickness ratio $L/t > 4$, and a fillet radius of $10/L$ (Fleischman and Sumer [23]). These optimum ratios were determined through an extensive analytical parameter study.

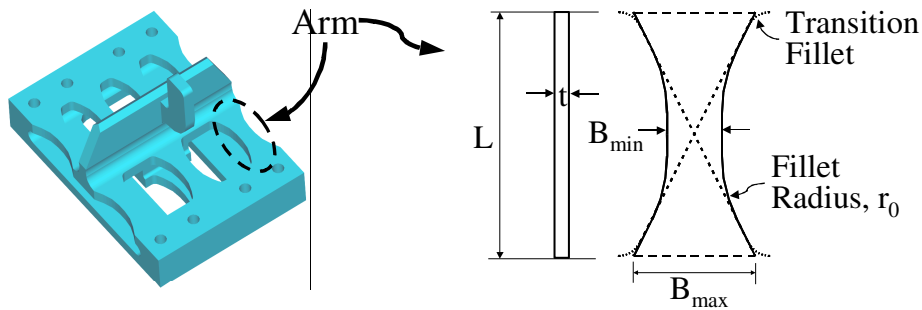


Figure 17. MC arm geometry parameters

Consider a MC arm, a WT section, and an ADAS element (Fig. 18a) of the same length and maximum width. Figure 18b shows the plastic strain distribution at a deformation demand corresponding to a W30 beam end rotation of 0.05 rad. A strain concentration is observed at the ends of the WT element. The ADAS geometry eliminates these hinges as is well documented (Whittaker et al. [22]), however, catenary forces create a strain concentration at the minimum section (Fig. 18b). In contrast, the MC geometry produces a relatively uniform plastic distribution along the arm, and at all locations below critical.

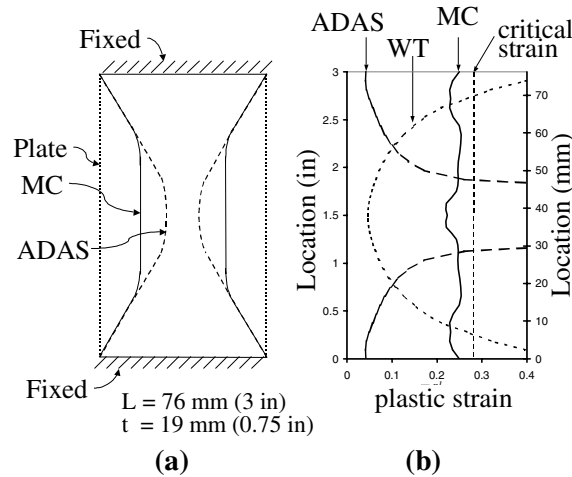


Figure 18. Distribution of equivalent plastic strain in WT, MC and ADAS.

Consider the length-to-thickness ratio required to obtain a uniform plastic strain distribution in the MC arm. Fig. 19a shows the strain distribution from FE analyses of different thickness MC arms at 0.05 rad. Fig. 19b shows plastic strain contours for the thinnest and thickest of the arms.

As seen, different relative thickness leads to different failure modes because thickness produces a different effect on flexural and axial response: the thick arm exhibits a shear/flexure mechanism while the thin arm exhibits a “necking” mechanism (Fleischman and Sumer [23]). Figure 19a shows that the shear/flexure mechanism produces concentrations at regions intermediate to the end and middle; conversely, the thin arm ($t = 0.5 \text{ in}$) exhibits no concentration of plastic strain at this displacement demand, only later forming the necking failure shown in Fig. 19c. As a result, a minimum length-to-thickness ratio of 4 is chosen for the MC arm geometry.

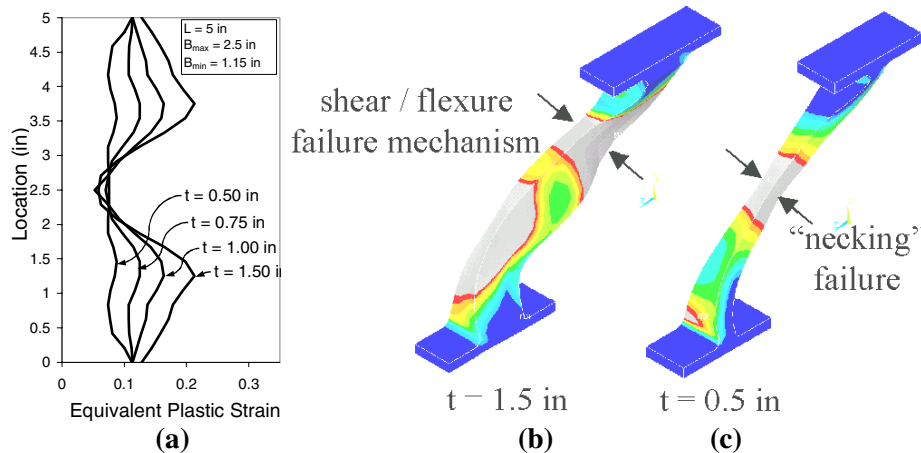


Figure 19. Plastic strain profile: (a) graph (0.05 rad); (b) shear/flexure mechanism; and (c) necking

The optimum arm geometry produces connectors of remarkable ductility. The MC geometry also eliminates bolt prying, greatly improving the efficiency and reliability of the connection, as shown through the experiment results.

Experimental Verification

The testing program involves two stages: In the pilot stage, isolated half-scale MC (Beta-1) prototypes and T-stub specimens of similar strength and stiffness were subjected to direct axial load. This loading is a simplification of actual conditions, however, it allows the MC concept to be verified rapidly and

economically. Following these proof of concept tests, the design was improved to a Beta-2 prototype shown in Fig. 15b.

Figure 20a shows the load vs. deflection comparison for monotonic tests of isolated MC and WTs. The MC achieves an extremely large ductility (0.085 rad. rotation for a 76 cm (30 in) deep beam). The MC has no bolt distress with a 2.2 cm (7/8 in) A325 bolt; contrast this with the failure of 2.9 cm (1.13 in) A490 bolts for the WT (shown in the inset of Fig. 20a with shear/flexure failure mechanism prediction).

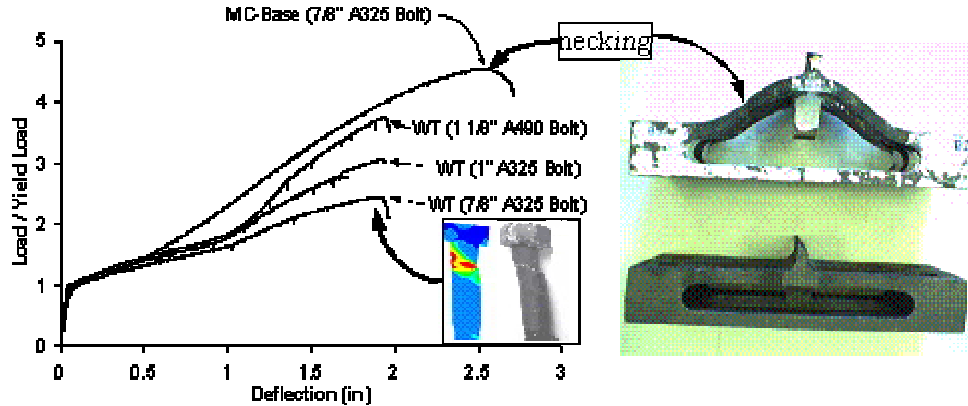


Figure 20: (a) Load vs. deflection and failed bolt in WT; (b) MC mechanism

The monotonic plot does not fully reveal the great advantage the MC possesses in low cycle fatigue life over the WT (even if bolt failure could somehow be avoided). This can be deduced from Fig. 21b, a strain plot at three specific regions (shown in Fig. 21a) vs. deflection (note the excellent agreement between the experiment and the analysis). Though the monotonic failure is necking of the arm at C, no plastic strain demand occurs there at $\theta < 0.024$ rad due to low catenary force at these demands. This implies that the MC low cycle fatigue life under expected ductility demands (0.03 rad) will be far superior because non-critical regions (A,E in Fig. 21a) undergo the larger cyclic plasticity. This outcome is evidenced in survival cycles of constant amplitude (0.72 in) tests of similar MC and WT (See Table 3). Note the WT bolts required to make this comparison. In the FEMA-350 test, the MC far exceeded qualifying drift capacities.

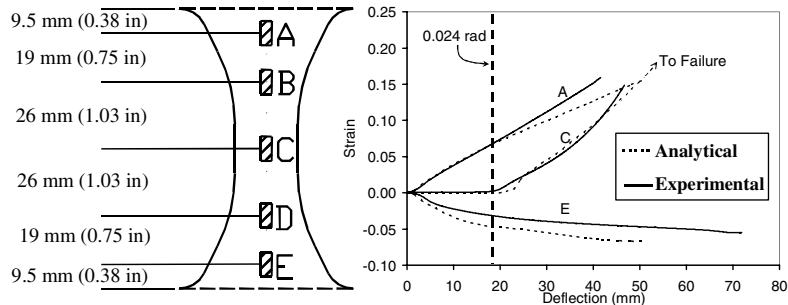


Figure 21. (a) Strain gage layout, (b) FE vs. test: Strain demand in MC arm.

Table 3. Selected MC Half -scale Test Descriptions

Test-ID	Type of Loading	Bolt diameter	Bolt material	Failure location	Max. stem displacement
MC-1	Monotonic	2.2 cm (7/8 in)	A325	arm	6.5 cm (2.6 in)
MC-2	FEMA-350	2.5 cm (1 in)	A325	arm	4.9 cm (1.9 in)
MC-3	Cyclic	2.2 cm (7/8 in)	A325	arm	1.8 cm (0.72 in) (44 times)
T-Stub-1	Monotonic	2.9 cm (1.13 in)	A490	bolt	4.9 cm (1.9 in)
T-Stub-2	Cyclic	2.9 cm (1.13 in)	A490	flange	1.8 cm (0.72 in) (19 times)

However, in the cyclic tests, the elongating of the arms in tension (as shown in Fig. 20b) create “truss action” on load reversal. High compressive forces are generated and a static “snap-through” occurs (point V in Fig. 22c). This phenomenon was accompanied by a torsional instability of the MC arms (See Fig. 22a), causing a slight loss of (compressive) load but more importantly strain amplification in high flexure regions (A or E) such that the ductility capacity was reduced. Fig. 22b shows the guide plate retrofit added to the Beta-1 prototype that eliminates the twisting mode. However; as they may be difficult to add as a cast feature, and extra fabrication steps are to be avoided, a Beta-2 configuration was developed.

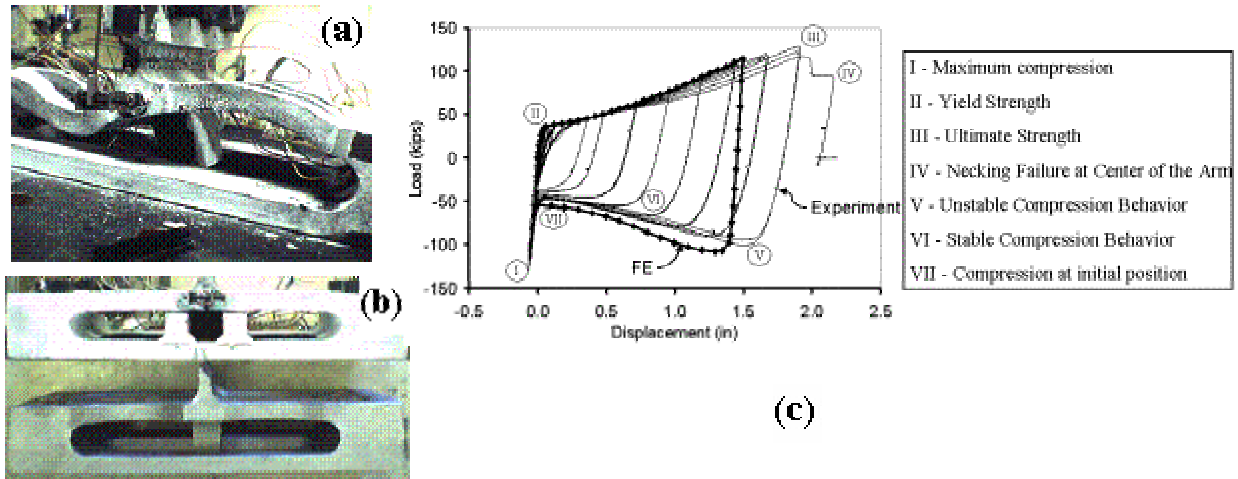


Figure 22. (a) Torsional mode, (b) Retrofitted MC, (c) Beta-1 prototype under FEMA-350 loading

Beta-2 Prototype

The response of the MC in a full connection is affected by several behaviors that were not fully captured in the isolated connector approach used to develop the Beta-1 prototype configuration. These behaviors include: (A) a trajectory that is not direct axial displacement but also contains transverse and rotational degrees-of-freedom that modify the strain distribution; (B) the associated shears and moments that develop at the MC stem which are determined by the indeterminate system of the top-and bottom connectors and web connection if present; forces that can impact the capacity design of both the column face bolts and the MC stem-to-beam flange weld; and, (C) a cyclic history that is determined in part by the instantaneous stiffness of the elements in the system and the contact condition of the MC under compression and can include instability modes.

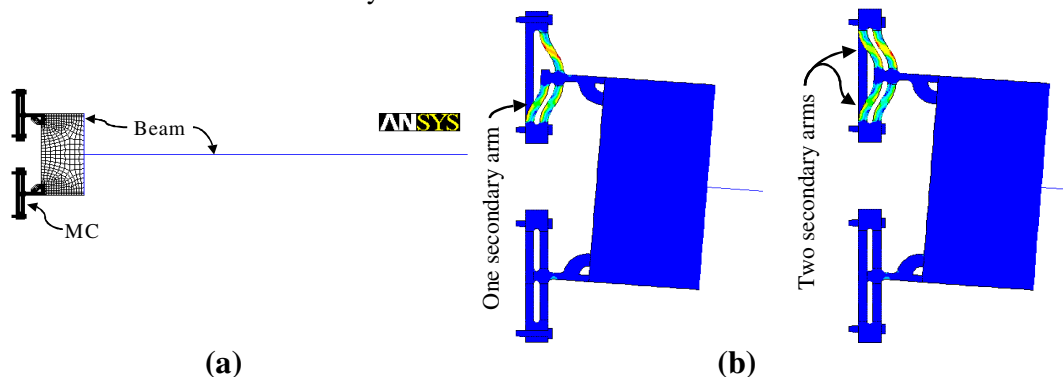


Figure 23. Beta-2 connection: (a) undeformed; (b) contour plots of alternative configurations

The second generation (Beta-2) prototype (See Fig. 15b) is a modified version of the Beta-1 prototype. The Beta-2, developed through cyclic analyses of the full connection, is better suited to interface the beam, maintain cyclic stability and handle indeterminate force conditions at the beam end. The analytical results from full connection model indicate that a second set of arms (parallel to the base) will both

mitigate the torsional instability and lessen the effects of the beam shear (See Fig. 23). The Beta-2 will be tested at full-scale in the ICEL test frame and design guidelines will be developed for a family of MCs.

CONCLUSIONS

Cast modular welded and bolted connections have been conceived, developed and tested. These connections exhibit superior ductility in comparison to traditional connections, stable and efficient energy dissipation, reliability and repeatability.

ACKNOWLEDGEMENT

This research was supported by NSF CAREER Award Grant CMS-01-96120; industry partners AISC and SFSA, including AISC member Able Steel Fabricators and SFSA member Varicast, Inc. ICEL laboratory provided by Intel, ConxTech, Inc., and ANSYS, Inc. The authors are grateful for this support.

Any opinions, findings, and conclusions or recommendations expressed in this material are those of the author(s) and do not necessarily reflect the views of the National Science Foundation.

REFERENCES

1. Malley, J. "SAC Steel Project: Summary of Phase 1 testing investigation results." *Engineering Structures*, 1998, 20(4-6): 148-162.
2. FEMA-350 "Recommended Seismic Design Criteria for New Steel Moment-Frame Buildings." 2000, by the SAC Joint Venture for the Federal Emergency Management Agency, Washington, DC.
3. Stojadinovic, B., Goel, S.C., Lee, K.H., and Margarian, A.G. "Parametric tests on unreinforced steel moment connections." *J. Struct. Engrg.*, 2000, ASCE, 126(1): 40-49.
4. ANSYS user's manual- ANSYS version 8.0, 2003, ANSYS Inc., Canonsburg, PA 15317
5. Monroe, R. "Steel Castings"; *Proceedings, 12th SFSA T&O Conf.*, Oct. 1995
6. Schneider, S.P., Amidi, A. "Seismic behavior of steel frames with deformable panel zone." *J. Struct. Engrg.*, ASCE, 1998, 124(1): 35-42.
7. Krawinkler, H., and Gupta, A. "Deformation and ductility demands in steel moment frame structures." *Stability and Ductility of Steel Structures*, T. Usami and Y Itoh, Editors, Pergamon, Elsevier Science Ltd., 1998: 167-178
8. El-Tawil, S. "Panel zone yielding in steel moment connections." *Engineering Journal*, Third Quarter, 2000: 120-131.
9. Englekirk, P.E. "Extant panel zone design procedures for steel frames are questioned" *Earthquake Spectra*, 1999, v.15, n.2, EERI, Oakland, California
10. Fleischman, R.B. and Li, X., "Development of Panel Zone Dissipator Modular Nodes for SMFs", submitted to *ASCE J. of Struc. Eng.*, 2003
11. FEMA-355C "State of the Art Report on System Performance of Steel Moment Frames Subject to Earthquake Ground Shaking", Sep. 2000, prepared by the SAC Joint Venture for the Federal Emergency Management Agency, Washington, DC.
12. International Building Code, March 2000, International Code Council.
13. Somerville, P., Smith, N., Punyamurthula, S., and Sun, J. "Development of Ground Motion Time Histories for Phase 2 of the FEMA/SAC Steel Project", SAC Background Document, 1997, Report No. SAC/BD-97/04
14. Coffin, L.F. "The flow and Fracture of Brittle material" *Jr. of Applied Mechanics*, vol. 17 (Trans. ASME, vol72), Sep. 1950: 233-248
15. Richard, R.M., Allen, J., and Partridge, J.E. "Accumulated Seismic Connection Damage Based upon Full Scale Low Cycle Fatigue Connection Tests", SEAOC Convention, 2001

16. Richard, R., Partridge, J.E., Allen, J., and Radau, S. "Finite Element Analysis and Tests of Beam-to-Column Connections," *Modern Steel Construction*, American Institute of Steel Construction, Chicago, Illinois, 1995, Vol. 35, No. 10: 44-47
17. Choi, J., Stojadinovic, B., and Goel, S.C., " Parametric Tests on the Free Flange Connection" Report SAC/BD-00/02, SAC Joint Venture, 2000
18. Choi, J.; Stojadinovic, B.; Goel, S.C. "Design of free flange moment connection" *Engineering Journal*, v 40, n 1, First Quarter, 2003: 25-41
19. Engelhardt, M. D., Winneberger, T., Zekany, A. J., and Potyraj, T. J. (1996). "Dogbone connection: Part II", *Modern Steel Construction*, 36(8), 46-55
20. Yang, T.S., and Popov, E. P. "Behavior of pre-Northridge moment resisting steel connections." Rep. No. UCB/EERC-95/08, 1995, Earthquake Engrg. Res. Ctr., Univ. of Calif., Berkeley, Calif.
21. Swanson, J.A., and Leon, R.T. "Bolted Steel Connections: Tests on T-Stub components." *J. Struc. Engrg.*, ASCE, 2000, Vol.126, No.1: 50-56
22. Whittaker, A.S., Bertero, V.V., Thompson, C.L., and Alonso L.J. "Earthquake Simulator Testing of Steel Plate Added Damping and Stiffness Elements", 1989, Report No. UCB/EERC-89/02 EQ Eng. Research Center, UCLA Berkeley.
23. Fleischman, R.B. and Sumer, A. "Optimum Arm Geometry for Ductile Modular Connectors", submitted to *ASCE J. of Struc. Eng.*, 2003